ACKNOWLEDGMENT

The authors wish to thank Prof. G. R. Krupholz for helpful comments and pointing out [13].

YUPING CHENG
School of Electrical and Electronic Engineering
Nanyang Technological University
Radar Lab S1-B4a-03
Singapore 639798

ZHENG BAO
PUFU ZHAO
Key Lab for Radar Signal Processing
Xidian University
Xian 710071
China

ZHIPING LIN
School of Electrical and Electronic Engineering
Nanyang Technological University
Singapore 639798

REFERENCES

[1] Skolnik, M. I. (1990)
Radar Handbook.
New York: McGraw-Hill, 1990.

[2] Wehner, D. R. (1994)
High Resolution Radar.
Boston, MA: Artech House, 1994.

[3] Scheer, J. A., and Kurtz, J. L. (1993)
Coherent Radar Performance Estimation.
Boston, MA: Artech House, 1993.

[4] Levanon, N., and Getz, B. (1994)
Comparison between linear FM and phase-coded CW radar.
IEE Proceedings—Radar, Sonar Navigation, **141**, 4 (Aug. 1994), 230–240.

[5] Baden, J. M., and Cohen, M. N. (1990)
Optimal peak sidelobe filter for biphase pulse compression.
In *Proceedings of IEEE International Radar Conference* (1990), 249–252.

[6] Cohen, M. N., Fox, M. R., and Baden, J. M. (1990)
Minimum sidelobe pulse compression codes.
In *Proceedings of IEEE International Radar Conference* (1990), 633–638.

[7] Kretschmer, F. F., and Welch, L. R. (2000)
Sidelobe reduction techniques for polyphase pulse compression codes.
In *Proceedings of IEEE International Radar Conference*, Alexandria, VA, May 2000, 416–418.

[8] Nunn, C. J., and Welch, L. R. (2000)
Multi-parameter local optimization for the design of superior matched filter polyphase pulse compression codes.
In *Proceedings of IEEE International Radar Conference*, Alexandria, VA, May 2000, 435–440.

[9] Skolnik, M. I. (1981)
Introduction to Radar Systems.
New York: McGraw-Hill, 1981.

[10] Viterbi, A. J., and Omura, J. K. (1979)
Principles of Digital Communication and Coding.
New York: McGraw-Hill, 1979.

[11] Cheng, Y. P., and Zhao, P. F. (1992)
The Doppler compensation for binary phase-coded waveforms.
Modern Radar (May 1992), 43–49.

[12] Cheng, Y. P., and Zhao, P. F. (1993)
The Doppler compensation for m-sequence phase-coded continuous waveforms.
Acta Electronic Sinica, **21**, 6 (1993), 40–45.

[13] Lank, G. W., Reed, I. S., and Pollon, G. E. (1973)
A semicoherent detection and Doppler estimation statistic.
IEEE Transactions on Aerospace and Electronic Systems, **AES-9**, 2 (Mar. 1973), 151–165.

[14] Viterbi, A. J. (1995)
CDMA: Principles of Spread Spectrum Communication.
Reading, MA: Addison-Wesley, 1995.

Characterizing Performance of α–β–γ Filters

The α–β–γ filter, a sampled data target tracker which can asymptotically track a constant acceleration target, is discussed in detail. The α, β, γ parameters are studied to characterize the stability of the filter and its performance viz its transient behavior. A closed-form equation for the mean square response of the system to white noise is derived. In addition, performance measures to gauge the transient response and the steady state tracking error are derived. The closed-form equations for the noise ratio and the transient and steady state error are exploited to optimally select the α, β, γ parameters. The resulting solutions are shown to reduce to some results presented in the literature for the α–β filter.

I. INTRODUCTION

Numerous applications such as air-traffic control, missile interception, and antisubmarine warfare require the use of discrete-time data to predict the kinematics of a dynamic object. The use of passive sonobuoys which have limited power capacity constrain us to implement target-trackers which are computationally inexpensive. It is with these considerations in mind, we analyze an α–β–γ filter to study its ability to predict the object kinematics in the presence of noisy discrete-time data.

There exists a significant body of literature which addresses the problem of *track-while-scan systems*. Sklansky [1] in his seminal paper analyzed the behavior of an α–β filter. His analysis of the range of the α–β smoothing parameters is based on the prediction characteristics, which resulted in a stable filter constraining the parameters to lie within

Manuscript received August 4, 2000; revised September 14, 2001, March 18 and May 9, 2002; released for publication May 9, 2002.

IEEE Log No. T-AES/38/3/06452.

Refereeing of this contribution was handled by P. K. Willett.

a stability triangle. He also derived closed-form equations to relate the smoothing parameters for critically damped transient response and the ability of the filter to smooth white noise, using a figure of demerit, which was referred to as the *noise ratio.* Finally he proposed, via a numerical example, a procedure to optimally select the α, β parameters to minimize a performance index, which is a function of the noise ratio and the tracking error for a specific maneuver. Following his work, Benedict and Bordner [2] used calculus of variations on the filter update equations to solve for an optimal filter, which minimizes a weighted function of the noise smoothing and the transient (maneuver following) response. They showed that the optimal filter is coincident with an α–β filter with the constraint that $\beta = \alpha^2/(2-\alpha)$. Simpson [3] extended this approach to an α–β–γ filter arriving numerically at the optimal condition $2\beta - \alpha(\alpha + \beta + 1/2\gamma) = 0$, which minimizes the update noise ratio and the transient response following a ramp and a quadratic input. Neal [4] later showed that Simpson's result is coincident with the steady state Kalman solution, and provided an additional optimal condition $\beta^2 = 2\alpha\gamma$ by assuming a random walk acceleration statistics. The α–β filter was also studied by Kanyuck [5] and Schooler [6] as a prediction filter in that the mean square error of the predicted position is addressed. Schooler derived a recursive algorithm to optimally select the α–β parameters, which was shown to be identical to the Kalman filter.

Since the development of the Kalman filter, which minimizes the unbiased mean square error estimation, numerous researchers applied the Kalman equations to the α–β–(γ) algorithm including various process noise models, i.e., discretized and discrete [7–10] white noise acceleration and exponentially correlated acceleration [11, 12]. Kalata [13] proposed a new parameter, which he referred to as the *tracking index* to characterize the behavior of the α–β–(γ) filters, and Ekstrand [14] parameterized the root-loci for the poles and zeros. The tracking index is defined as the ratio of the position maneuverability uncertainty to the position measurement uncertainty, which fully describes the optimal set of the α–β–γ parameters. An alternative algorithm avoiding complex polynomial root evaluations is given by Gray and Murray [15]. The two-stage Kalman estimator developed by Alouani [16], Xia [17], and Rice and Blair [18] tracks maneuvering targets by introducing an acceleration bias in the dynamic model. Furthermore, the second stage can be augmented by kinematic constraints, for example constant speed targets as shown by Blair [19].

A detailed analysis of the α–β–γ filter is carried out in this report. Section II discusses the bounds on the smoothing parameters for a stable filter and demarcates the underdamped and overdamped region of the stability volume. This is followed by a closed-form derivation of the prediction noise ratio for the α–β–γ filter in Section IIIA. In Section IIIB, a closed-form expression for the steady state errors and a performance measure to gauge the transient response of the filter are derived followed by optimization of the smoothing parameters for various cost functions (maneuvers and noise ratios) in Section IV. The paper concludes with some remarks in Section V.

II. STABILITY ANALYSIS

The α–β–γ tracker is a one-step ahead position predictor that uses the current error, called the innovation, to predict the next position. The innovation is weighted by the smoothing parameter α, β, and γ. These parameters influence the behavior of the system in terms of stability and ability to track the target. Therefore, it is important to analyze the system using control theoretic aspects to gauge its stability and performance.

The one-step ahead prediction equation for the α–β–γ tracker is:

$$x_p(k+1) = x_s(k) + Tv_s(k) + \tfrac{1}{2}T^2a_s(k) \tag{1}$$

and the velocity of the target is predicted by the equation:

$$v_p(k+1) = v_s(k) + Ta_s(k) \tag{2}$$

where the smoothed kinematic variables are calculated by weighting the innovation as follows:

$$x_s(k) = x_p(k) + \alpha(x_0(k) - x_p(k)) \tag{3}$$

$$v_s(k) = v_p(k) + \frac{\beta}{T}(x_0(k) - x_p(k)) \tag{4}$$

$$a_s(k) = a_s(k-1) + \frac{\gamma}{2T^2}(x_0(k) - x_p(k)). \tag{5}$$

The observation at time k is denoted by $x_0(k)$.

Applying the z-transform to (1) to (5) and solving for the ratio x_p/x_0 leads to the prediction transfer function in z-domain, which is:

$$G(z) = \frac{(\alpha+\beta+\frac{1}{4}\gamma)z^2 + (-2\alpha-\beta+\frac{1}{4}\gamma)z + \alpha}{z^3 + (\alpha+\beta+\frac{1}{4}\gamma-3)z^2 + (-2\alpha-\beta+\frac{1}{4}\gamma+3)z + \alpha - 1}. \tag{6}$$

Equation (6) can now be studied to determine the bounds of α, β and γ for stability. For the third order system, the *Jury's Stability Test* is used, to determine the region of stability, resulting in the parameter constraints:

$$0 < \alpha < 2 \tag{7a}$$

$$0 < \beta < 4 - 2\alpha \tag{7b}$$

$$0 < \gamma < \frac{4\alpha\beta}{2-\alpha}. \tag{7c}$$

Details of the development are included in Appendix A.

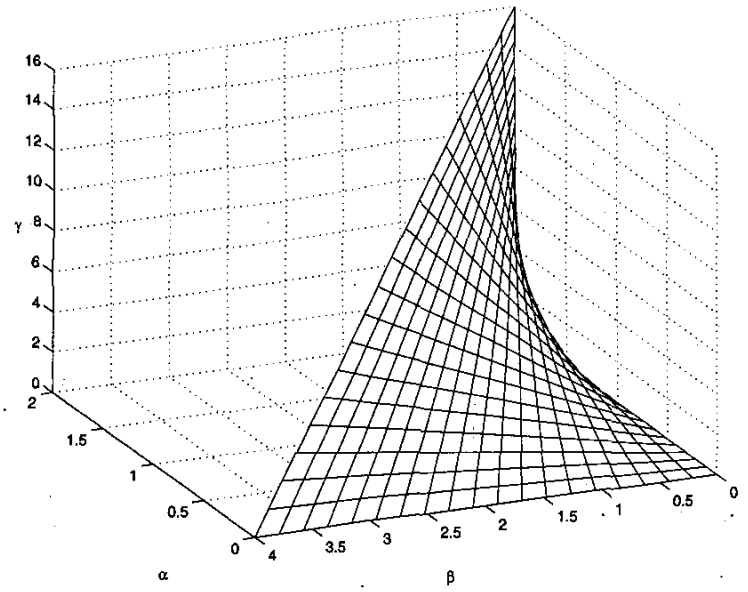

Fig. 1. Stability volume of α–β–γ tracker.

Fig. 1 illustrates the bounding surfaces of (7), which circumscribe the stability volume in the α–β–γ space, where (7a) and (7b) span the stability triangle in the α–β plane and (7c) limits γ.

It is desirous to divide the stability volume into regions which are characterized by specific classes of transient responses such as underdamped, overdamped, and critically damped. However, the difficulty in factoring the characteristic polynomial of the transfer function in the α–β–γ space prompt us to conceive of a new space which we refer to as the a-b-c space. In this space, the characteristic polynomial is represented as

$$(z + c)(z^2 + (a + b - 2)z + 1 - a) \tag{8}$$

where the second-order factor has a form which is identical to the characteristic equation of the α–β filter and the third pole at $-c$ is real. The above transformation might be understood as a partial pole placement incorporating intuitive knowledge about the second-order α–β filter. Comparing the denominator of (6) with (8), the following transformation is derived

$$\begin{aligned} \alpha &= 1 + c(1 - a) \\ \beta &= a(1 + c) + \tfrac{1}{2}b(1 - c) \\ \gamma &= 2b(1 + c). \end{aligned} \tag{9}$$

From the remaining paper, the usefulness of this transformation becomes evident. For example, when one derives the stability volume of the α–β–γ filter since c is constrained to lie in the interval $[-1\ 1]$, and the a-b space resembles the α–β space, the stability volume in the a-b-c space is a prism (Fig. 2) with a triangular cross section, which is derived from the α–β filter. Mapping the stability prism in the a-b-c space to the α–β–γ space using (9), we rederive the stability volume illustrated in Fig. 1.

Since, the pair of poles of (8), which are functions of a and b, are responsible for the second-order response of the system, the a-b-c space is divided by extruding the lines which divide the stability triangle of the α–β filter, in the c dimension. These surfaces, shown in Fig. 2, are transformed using (9) to the α–β–γ space. Fig. 3 shows the surface in the α–β–γ space corresponding to a pair of coincident poles. It is clear that the surface in Fig. 3 separates the stable region into different sectors, which are difficult to visualize compared with Fig. 2.

Similarly, the remaining surfaces in the a-b-c space can be mapped into the α–β–γ space. These mappings illustrate the fact that for $\gamma = 0$, the third-order tracker reduces to the α–β tracker. Substituting $\gamma = 0$ in the transfer function (6), results in a pole zero cancellation at $z = 1$, resulting in a second order tracker. From (9), we can infer that c equals -1 when $\gamma = 0$, and furthermore a and b degenerate to α and β. The cross section at $c = -1$ therefore corresponds to the α–β tracker. Note that $c = 0$ does not result in the α–β–γ degenerating to the α–β filter.

III. PERFORMANCE OF TARGET TRACKER

A. Noise Ratio

Measurement noise significantly effects the performance of target trackers. It is therefore, of interest to characterize the noise filtering strengths of the tracker, which can be described by the noise ratio. In this section, we derive a closed-form expression for the prediction and smoothing (update) noise ratio in terms of the α, β, and γ parameters.

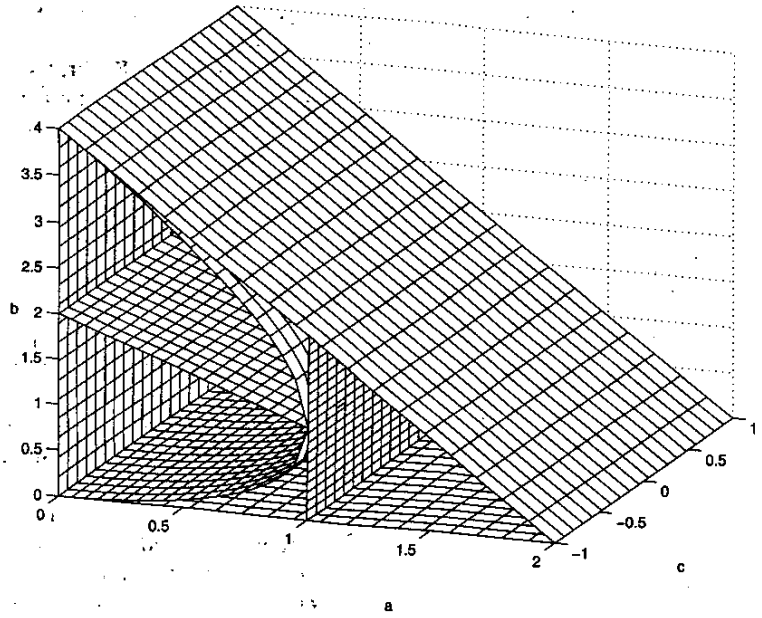

Fig. 2. Stability prism in a-b-c space, where cross section of a-b plane resembles stability triangle.

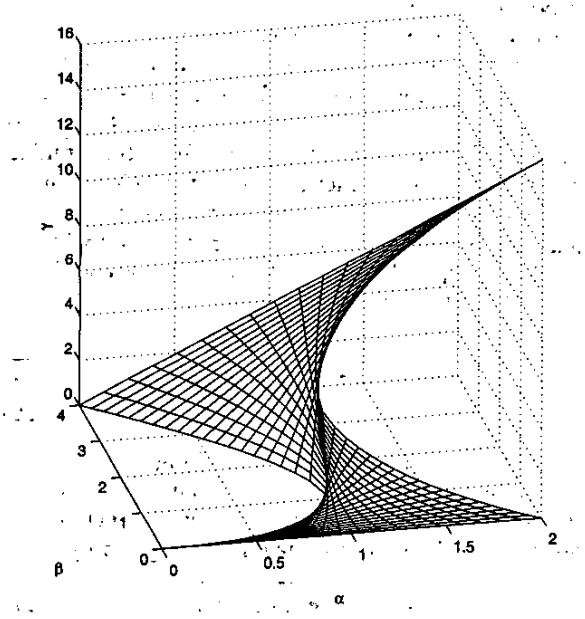

Fig. 3. Coincident pole pair surface in α–β–γ space.

Studying the effect of noisy signals requires a performance measure gauging the influence of the noise on the system. Since the response of the system to a noisy input can reflect this influence, the *noise ratio* is defined as the ratio of the rms value of the system response to the rms value of the noisy input. Depending on the purpose of the target tracker, different system responses have been considered. The noise ratio ρ_* is defined as

$$\rho_* \equiv \sqrt{\frac{\overline{x_*^2(t)}}{\overline{x_0^2(t)}}} \tag{10}$$

where the subscript $*$ represents the update noise ratio ρ_s or the prediction noise ratio ρ_p. Since we require the tracker to reject measurement noise, a small value of ρ_* implies an excellent filtering of noise. In particular, the update noise ratio should be less than one to alleviate the input noise.

The rms value in (10) is a consistent[1] estimator of the second-order moment, and the definition of the noise ratio can be restated in terms of expectations denoted by $E\{\cdot\}$

$$\rho_* = \sqrt{\frac{E\{x_*^2\}}{E\{x_0^2\}}}. \tag{11}$$

The input noise is modeled as discrete Gaussian white noise with zero mean such that the second-order moment $E\{x_0^2\}$ results in the variance of the input noise σ_0^2. The second-order moment of the prediction and the update position can be derived by rewriting (1)–(5) in state space as

$$\mathbf{z}_s(k) = \mathbf{z}_p(k) + K(x_0(k) - C\mathbf{z}_p(k)) \tag{12}$$

$$\mathbf{z}_p(k+1) = \Phi\mathbf{z}_s(k) \tag{13}$$

where $\mathbf{z}_p$ is the state vector $[x_p\ v_p\ a_p]^T$, and the corresponding transition matrix Φ is defined by

$$\Phi = \begin{bmatrix} 1 & T & \frac{1}{2}T^2 \\ 0 & 1 & T \\ 0 & 0 & 1 \end{bmatrix}.$$

[1]A consistent estimator $\hat{\Theta}$ converges to the true value θ as sample size increases [20].

The gain K and the output matrix C obtained by the prediction equations evaluate to:

$$K = \left[\alpha \ \frac{\beta}{T} \ \frac{\gamma}{2T^2}\right]^T, \qquad C = [1 \quad 0 \quad 0].$$

The predicted and smoothed position are the first element of the vector $\mathbf{z}_p$ and $\mathbf{z}_s$, respectively, which can be calculated as:

$$x_p(k+1) = C\mathbf{z}_p(k+1) \tag{14}$$

$$x_s(k+1) = C\mathbf{z}_s(k+1). \tag{15}$$

Substituting (13) and (14) into the second-order moment of the prediction, and defining the covariance matrix of the state $\mathbf{z}_p$ by $\hat{P}$ yields the dynamic equation for $\hat{P}$

$$\begin{aligned} E\{\mathbf{z}_p(k+1)\mathbf{z}_p^T(k+1)\} &= \hat{P}(k+1) \\ &= \Phi(I-KC)\hat{P}(k)(I-KC)^T\Phi^T \\ &\quad + \Phi K\sigma_0^2 K^T\Phi^T \end{aligned} \tag{16}$$

$$E\{x_p^2(k+1)\} = C\hat{P}(k+1)C^T. \tag{17}$$

The square of the prediction noise ratio is the element $\hat{P}_{1,1}$ divided by the input noise variance, as the solution of (17) reaches the steady state Appendix B, which yields:

$$\rho_p^2 = \frac{2\alpha^2+\alpha\beta+2\beta}{\alpha(4-2\alpha-\beta)} + \frac{4\beta\gamma}{\alpha(4-2\alpha-\beta)(4\alpha\beta+\alpha\gamma-2\gamma)}. \tag{18}$$

Similarly, the square of the update noise ratio can be calculated as:

$$\rho_s^2 = \frac{2\alpha^2-3\alpha\beta+2\beta}{\alpha(4-2\alpha-\beta)} + \frac{4\beta\gamma(1-\alpha)^2}{\alpha(4-2\alpha-\beta)(4\alpha\beta+\alpha\gamma-2\gamma)}. \tag{19}$$

The constant noise ratio surface typically displayed as a function of the square of the noise ratio $\rho_p^2 = 10$ is shown in Fig. 4(a) and for $\rho_s^2 = 0.8$ in Fig. 4(b). As mentioned in Section II, the α–β–γ filter reduces to a two-parameter tracker if γ becomes zero. Thus, the noise ratio of the α–β filter can easily be extracted from (18). The line of constant noise ratio for the α–β filter is also included in Figs. 4 by setting $\gamma = 0$. However for greater clarity, the curves of constant noise ratio in the α–β space are shown in Fig. 5(a) and Fig. 5(b) for various noise ratios. One can observe that with increasing values of β the noise transmission increases and that for a fixed β, a matching α exists, which minimizes the noise ratio. The constant ρ_s curves are skewed to the right of the constant ρ_p curves, which implies that the appropriate noise ratio should be used in the optimization based on whether the filter objective is prediction or estimation. The dashed-dot and dashed lines in Fig. 5(b) enclose the α–β region, which corresponds to an update noise ratio less than one.

The α–β part of (18) differs from that derived by Sklansky [1] and the α–β part of (19) conforms with the variance reduction ratio developed by Benedict and Bordner [2].

B. Prediction Error

Numerous cost functions can be used to gauge the performance of a tracker, such as the steady state tracking error, the transient response of the tracker, and the noise ratio, besides others. In this work, we endeavor to derive closed form expressions for the steady state errors and the sum of the square of the errors, which capture the transient behavior of the α–β–γ filters for two classes of trajectories. The first is a circular trajectory with the target moving at constant speed and the second is a straight line trajectory where the target moves with constant acceleration. These measures can then be exploited to determine optimal sets of parameters for any cost function, which are weighted combinations of these performance measures.

The tracking error is defined as the difference between the observed and the predicted position, and its discrete transformation needs to be derived. The innovation in the smoothing equations (3), (4), and (5) represents the maneuver error of the filter. Substituting the innovation with the term $e(k)$, and transforming the prediction equation (1) and the smoothing equations (3), (4), and (5) into the z-domain, yields the relationship between the maneuver error and the observed position, which is

$$e_{\alpha\beta\gamma} = \frac{(z-1)^3 x_0}{z^3 + (\alpha+\beta+\frac{1}{4}\gamma-3)z^2 + (-2\alpha-\beta+\frac{1}{4}\gamma+3)z + \alpha - 1}. \tag{20}$$

1) *Circular Trajectory*: The tracking error of a filter following a circular trajectory can be resolved into components e_x and e_y in the x and y directions, respectively. The net error magnitude is given by

$$e(t) = \sqrt{e_x^2(t) + e_y^2(t)}. \tag{21}$$

Assuming that the target traces a circular path with radius R while moving at constant speed, results in a constant angular velocity. The target's position can be described in the time domain using the projection of a rotating phasor, via the cosine and sine function, which also can be mapped into the complex domain as

$$\begin{aligned} x_0(t) &= Re^{j\omega t} \\ y_0(t) &= jRe^{j\omega t} \end{aligned} \tag{22}$$

where the y axis has been swapped to lead the x axis. Substituting the discrete transformation of the input $x_0(t)$ and $y_0(t)$ into the z-transformation of the error (equation (20)) and substituting $z = e^{j\omega T}$, the steady

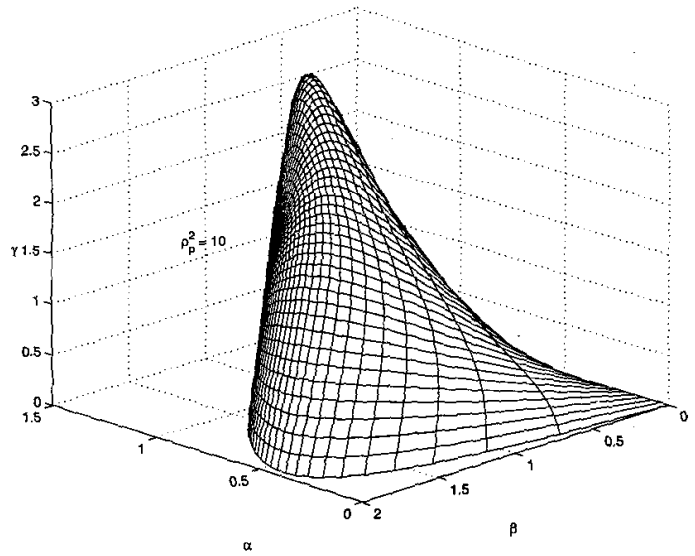

(a)

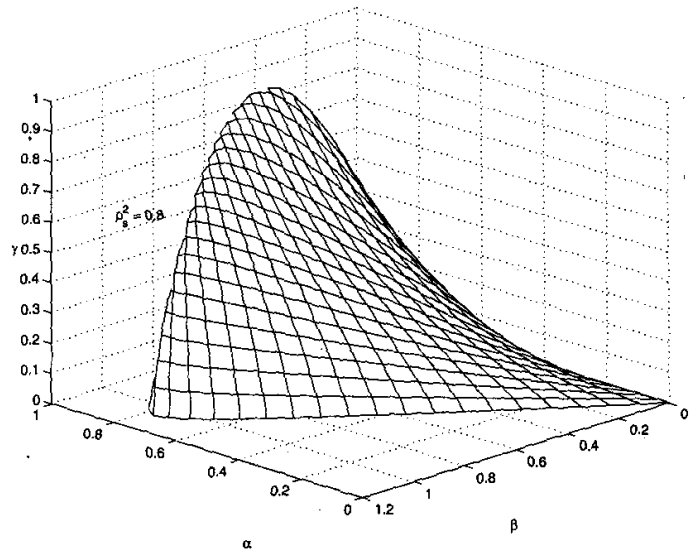

(b)

Fig. 4. Constant ρ_*^2 surfaces in α–β–γ space. (a) Prediction noise ratio ρ_p. (b) Update noise ratio ρ_s.

state values of the errors can be represented as

$$\begin{aligned} e_x(nT) &= Re_{\alpha\beta\gamma}(e^{j\omega T})e^{j\omega nT} = \hat{R}e^{j(\omega nT+\psi)} \\ e_y(nT) &= jRe_{\alpha\beta\gamma}(e^{j\omega T})e^{j\omega nT} = j\hat{R}e^{j(\omega nT+\psi)} \end{aligned} \tag{23}$$

where $\hat{R} = |Re_{\alpha\beta\gamma}(e^{j\omega T})|$, $\psi = \arg\{Re_{\alpha\beta\gamma}(e^{j\omega T})\}$.

Equation (23) states that the magnitude of the maneuver error for a circular path is constant at all sampling instants, and only the phase changes with each time step. To derive an expression for the tracking error for an α–β–γ filter, we substitute the corresponding discrete transformation $e_{\alpha\beta\gamma}(e^{j\omega T})$ into (23). The maneuver error of a circular target path of an α–β–γ tracker can now be simplified to

$$e = \frac{4R\sin^3\left(\frac{\omega T}{2}\right)}{\sqrt{\sin^2\left(\frac{\omega T}{2}\right)[((2-\alpha)\cos\omega T + \alpha + \beta - 2)^2 + \alpha^2\sin^2\omega T] + \gamma\left(\frac{\gamma}{32}(\cos\omega T + 1) - \frac{\alpha}{4}\sin^2\omega T\right)}}. \tag{24}$$

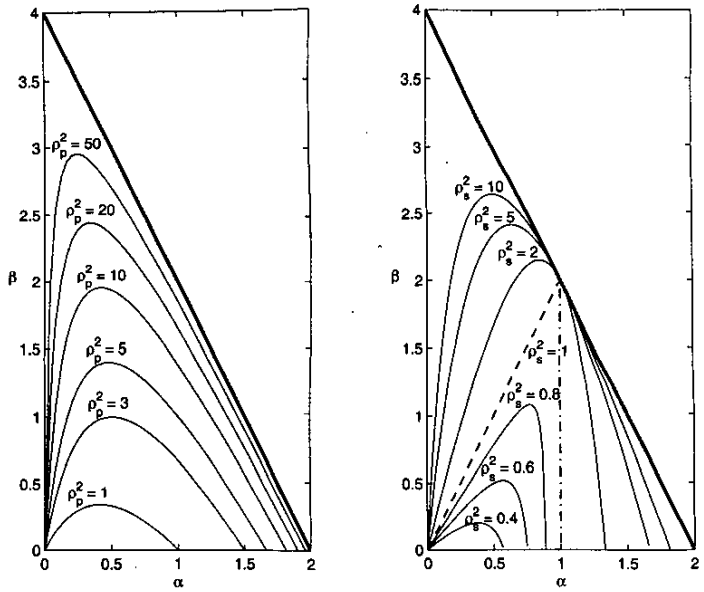

Fig. 5. Constant ρ_*^2 curves in stability region of α–β tracker. Stability region enclosed by coordinate axes and line $\beta = 4 - 2\alpha$. (a) Prediction noise ratio ρ_p. (b) Update noise ratio ρ_s.

To determine the steady state error for an α–β filter, we can substitute the corresponding error function $e_{\alpha\beta}(e^{j\omega T})$ into (23), or set γ to zero in (24). This leads to the maneuver error of the α–β filter

$$e = \frac{4R\sin^2\left(\frac{\omega T}{2}\right)}{\sqrt{[(2-\alpha)\cos\omega T + \alpha + \beta - 2]^2 + \alpha^2\sin^2\omega T}} \tag{25}$$

where the maneuver error of the α–β filter is the same as the closed form expression derived by Sklansky [1]. Sklansky [1], proposed simplifying the expression for $\omega T \ll \pi$ by neglecting the term under the radical, reducing (25) to

$$e \approx \frac{a_r T^2}{\beta} \tag{26}$$

where a_r is the centripetal acceleration given by $R\omega^2$.

2) *Straight Line Maneuvers*: Besides the circular maneuver, the straight line maneuver is one which needs to be studied carefully. This section presents the derivation of closed form expressions for steady state errors and the sum of the square of the errors for α–β and α–β–γ filters.

Unlike the derivation of the error for the circular path, the error for a straight line trajectory can be simplified by assuming that the target path is coincident with one of the reference axis, reducing the problem to a single dimension. Assuming constant acceleration along the straight line with zero initial position, the targets position is given by:

$$x_0(t) = \frac{1}{2}a_s t^2 + vt \Leftrightarrow x_0(z) = \frac{a_s T^2 z(z+1)}{2(z-1)^3} + \frac{vTz}{(z-1)^2} \tag{27}$$

where a_s is the acceleration and v is the initial velocity. The choice of constant acceleration is made to illustrate the ability of a higher order tracker to track the target without a steady state error. Simulating the α–β tracker for this maneuver, results in a steady state error, in contrast to the α–β–γ tracker, which exhibits no steady state error. Similar to the derivation of (23), the maneuver error for a straight line is obtained by substituting the z-transform of x_0 into (20). The maneuver error for the α–β tracker and the α–β–γ trackers are

$$e_{\alpha\beta} = \frac{\frac{1}{2}a_s T^2 z(z+1) + vTz(z-1)}{(z^2 + (\alpha+\beta-2)z + 1 - \alpha)(z-1)}, \tag{28}$$

$$e_{\alpha\beta\gamma} = \frac{\frac{1}{2}a_s T^2 z(z+1) + vTz(z-1)}{z^3 + (\alpha+\beta+\frac{1}{4}\gamma-3)z^2 + (-2\alpha-\beta+\frac{1}{4}\gamma+3)z + \alpha - 1}. \tag{29}$$

The steady state error is obtained by applying the final value theorem [21] to (28) and (29), which for the α–β tracker leads to the interesting result,

$$e_{\alpha\beta}(t \to \infty) = \frac{a_s T^2}{\beta} \tag{30}$$

which is coincident with the maneuver error for a circular path with a high sampling rate, as derived by Sklansky [1] (equation (26)). As can be seen from (29), the steady state error of the α–β–γ tracker

$$e_{\alpha\beta\gamma}(t \to \infty) = 0 \tag{31}$$

vanishes for the case of constant acceleration.

3) *Transient Response Performance Measure*: The transient response can be characterized by a performance measure which is defined as the sum of the square of the tracking errors as time tends to infinity. This measure can be defined in discrete time as

$$J = \sum_{k=0}^{\infty} Te^2(k) \tag{32}$$

which can be calculated by simulating the response of the system given in (28) and (29), and summing the resulting error $= u - y$, where y is the system response and u is the true target position. Instead, of using simulations, a closed-form expression can be derived using *Parseval's Theorem* [21]. Rewriting (32) and using *Parseval's Theorem* and the *Residue Theorem* we have

$$\frac{J}{T} = \frac{1}{2\pi j}\oint_C e(z)e(z^{-1})z^{-1}dz = \sum_{\nu=1}^{p}\operatorname*{Res}_{z_\nu}[e(z)e(z^{-1})z^{-1}] \tag{33}$$

where the line integral is carried out along a closed curve C, which is also given by the sum of the residues at the singular points within the closed curve C. The closed curve C is the unit circle which includes all the stable poles of $e(z)$.

As shown in (30), the α–β tracker exhibits a non-zero final value, so that the performance measure defined in (32) is not finite. However, subtracting the steady state error from the transient error yields a finite solution for the cost function. To derive the finite cost characterizing the transient behavior of the α–β filter tracking a constant acceleration profile, the z-transform of the augmented discrete error is:

$$e_{\alpha\beta}(z) = \frac{\frac{1}{2}a_sT^2z(z+1) + vTz(z-1)}{(z^2 + (\alpha+\beta-2)z + 1 - \alpha)(z-1)} - \frac{a_sT^2}{\beta}\frac{z}{z-1} \tag{34}$$

where the z-transform of the steady state error is subtracted from the original error function. Solving (33) by determining the residues of the three poles of $e_{\alpha\beta}(z)$ yields a closed-form equation for the cost function of the α–β tracker

$$J_{\alpha\beta} = \frac{v^2T^3(\alpha-2)}{\alpha\beta(2\alpha+\beta-4)} + \frac{\frac{1}{4}a_s^2T^5(2\beta+\alpha\beta+2\alpha^2)}{\alpha\beta^3} - \frac{va_sT^4}{\beta^2}. \tag{35}$$

The first expression in (35) is the transient cost function, corresponding to a constant velocity target motion referenced as $J_{\alpha\beta,v}$. The second expression corresponds to the cost for a target path, which is parameterized by constant acceleration and zero initial velocity referenced as $J_{\alpha\beta,a}$. The third term is due to the steady state error as aforementioned.

Since the α–β–γ filter tracks the target without steady state error, the cost defined in (32) is finite. Thus, the cost function of an α–β–γ tracker for an accelerating target along the straight line given in (33) is obtained by using the error function (29). Since the derivations of the cost function in the α–β–γ space are more complex than in the a-b-c space, (29) is transformed to the a-b-c space, where the discrete error transformation becomes:

$$e(z) = \frac{\frac{1}{2}a_sT^2z(z+1) + vTz(z-1)}{(z+c)(z^2 + (a+b-2)z + 1 - a)}. \tag{36}$$

A closed-form expression of the cost function is now obtained in the a-b-c space

$$J_{abc} = \frac{2(c - ca - 1)T^3v^2}{a(2a+b-4)(c-1)[c(a+b+ca) - (1-c)^2]} + \frac{\frac{1}{2}a_s^2T^5(c(a-1)-1)}{ab(1+c)[c(a+b+ca) - (1-c)^2]}. \tag{37}$$

Like the α–β filter, the first term is the contribution to the measure of the tracker's performance for a constant velocity input ($J_{abc,v}$), and the second term represents the cost for a constant accelerating target ($J_{abc,a}$). Equation (37) cannot be reduced to an α–β tracker by substituting c with -1, since this results in the second term being divided by zero, resulting in an infinite value for $J_{\alpha\beta\gamma}$ which is consistent with our intuition, since the integral over infinite time of a constant value is infinity.

The different performance measures defined in (24), (35), and (37) can now be used in an optimization process to optimally select a set of smoothing parameters α, β, and γ for a specific maneuver.

IV. DESIGN OF OPTIMAL FILTERS

We have derived regions of stability for the α–β and the α–β–γ filters. The selection of the smoothing parameters within the region of stability is a function of the trajectory of the target, the noise in the measurement, the steady state error, and the transient response of the filter. To arrive at the optimal set of parameters, a constrained parameter optimization problem is formulated. This is feasible since closed-form expressions for various performance measures have been derived in Sections IIIA and IIIB. Furthermore, closed-form solutions for the optimal parameter are derived for a set of target trajectories.

Define a figure of demerit which consists of two terms: the first is a function of the tracking error, and the second is a function of the noise ratio. This provides us with the flexibility to include steady state error, transient error, etc. and permits us to weight them based on their importance. In the proceeding text κ is a weighting factor to penalize the contribution of one term relative to the other. The constraints for

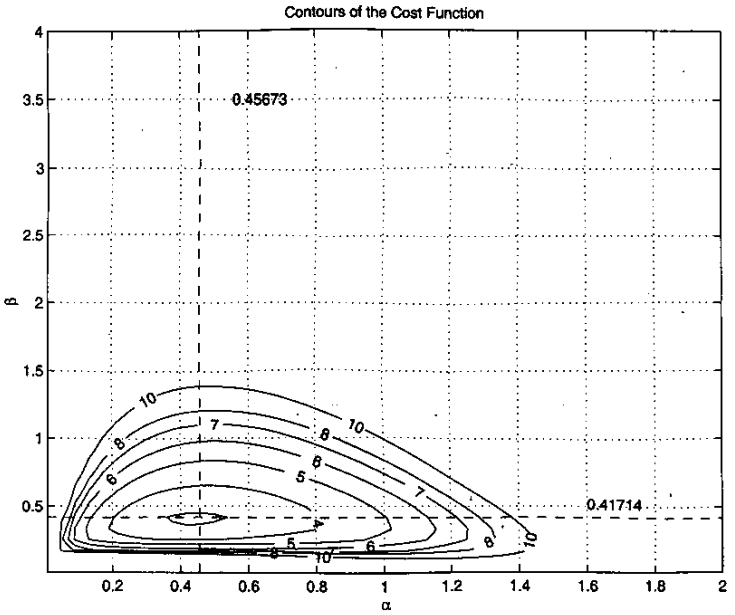

Fig. 6. Contours of cost function for α–β filter with $\kappa = 0.01$ including minimum value.

the optimization are defined by the stability region of the tracker. As shown in Section IIIB, there are different measures to capture the tracking error for specific maneuvers, such as straight line or circular target path. The maneuver error can be characterized by transient response and/or the steady state error. The choice of the appropriate cost function depends on the optimization purpose.

A. Circular Trajectory

The first task attempted in this work was an extension of the optimization of a cost defined by Sklansky [1] for the design of filters for tracking submarines. To study the variation of the smoothing parameters as a function of the relative importance of the steady state error for a circular maneuver and the prediction noise ratio, a series of optimizations were carried out. Thus a cost function can be designed with the maneuver error (25) and the square of the noise ratio (18)

$$J = e^2 + \kappa \rho_p^2 \overline{x_0^2}. \tag{38}$$

Assuming that the smallest turn radius of a submarine travelling with a speed of $v = 3$ knots is 45 m, leads to the angular velocity of $\omega = v/R = 0.034$ rad/s. Assume that the variance of the measurement noise is 200 m^2, and weight the noise ratio by κ in (38). The contours of the cost function (equation (38)) are illustrated in Fig. 6, where $\kappa = 1/100$ and the sampling rate is assumed to be $T = 3$ s. The contour plot illustrates the location of the minima. To illustrate the effect of changing the weighting parameter, a series of optimizations are carried out and the resulting set of α–β parameters are plotted. Fig. 7(a) illustrates that the optimal set of parameters monotonically decrease with an increase of κ. It can be seen that for large values of the weighting factor, the smoothing parameters asymptotically tend to $\alpha = 0.0032$ and $\beta = 0$, which can be shown by setting the maneuver error in the cost function to zero and solving for the optimal α–β parameters. The shape of the curve does not change for circular maneuvers of different radii, since the increase in the radius of the trajectory is equivalent to increasing the weighting factor. The optimal smoothing parameters are displayed in the α–β space in Fig. 7(b), where the cost function is a weighted combination of the noise ratio and the steady state maneuver error when the target follows a circular path. Fig. 7(b) shows various values of the weighting factor κ along the line of optimal solutions. It can be seen that the optimal solutions lie in the underdamped region only.

Extending the same procedure to an α–β–γ tracker, leads to similar results for the optiimal smoothing parameter. The change of the parameters versus the weighting factor is shown in Fig. 8.

B. Straight Line Maneuver

In practice the tracker rarely reaches steady state because the target path is continuously changing. Including the transient response of the tracker to the cost function leads to a more realistic performance measure. Section IIIB contains the development of the transient error cost function for tracking a straight path. A closed-form solution is given for an α–β tracker (equation (35)), and an α–β–γ tracker (equation (37)). Depending on the path of the target, the tracker can exhibit a steady state error. We can now modify

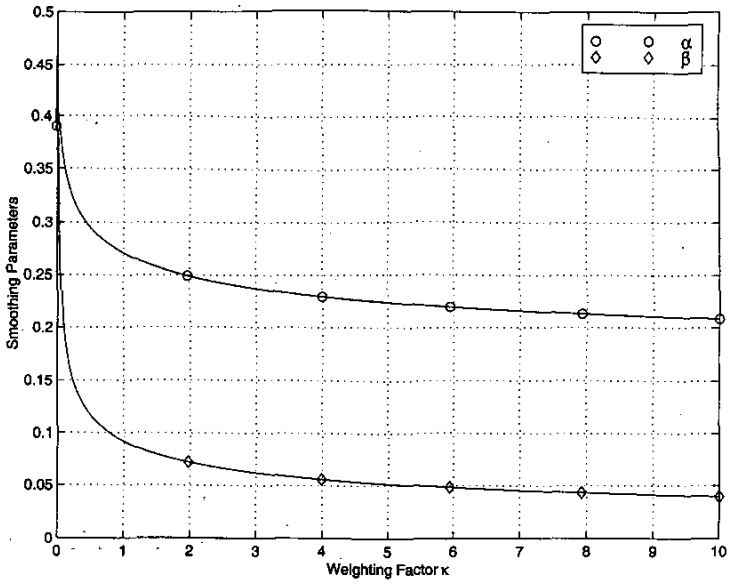

(a)

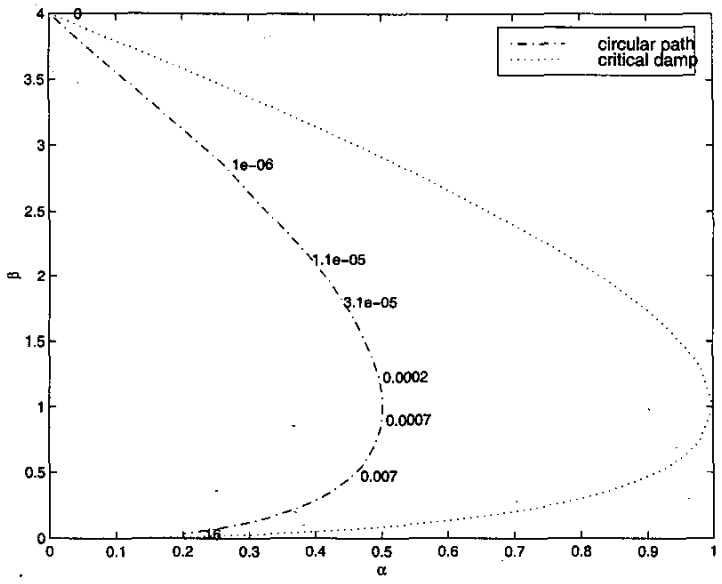

(b)

Fig. 7. Optimal solution of α and β for tracking a circular path. (a) Optimal parameters as function of κ. (b) In α–β space, where κ is labeled on optimal curve.

(38) by including the performance measure gauging the transient performance, as follows:

$$f = J_{\alpha\beta(\gamma)} + \kappa_{ss} e^2_{\alpha\beta(\gamma)}(t \to \infty) + \kappa\rho^2\overline{x_0^2} \qquad (39)$$

where $J_{\alpha\beta(\gamma)}$ is the transient error cost and $e^2_{\alpha\beta(\gamma)}(t \to \infty)$ the steady state error of the α–β tracker or the α–β–γ tracker. The weighting factor κ_{ss} adjusts the influence for the steady state error. The transient error cost function in (35) and (37) are sorted as a function of velocity and acceleration. The effect of the velocity and acceleration on the optimal set of the smoothing parameter of an α–β tracker is shown in Fig. 9 for three cost functions. The three curves in the graph correspond to objective functions which weigh the noise ratio to the tracking errors for targets moving with constant velocity, constant acceleration, and the steady state tracking error for a constant acceleration input.

The solid line in Fig. 9 exhibits variation of the optimal parameters as a function of the weighting parameter for targets with constant velocity. A closed-form expression of this optimal curve can be derived as described by the following algorithm. The objective function (equation (39)) for the proposed

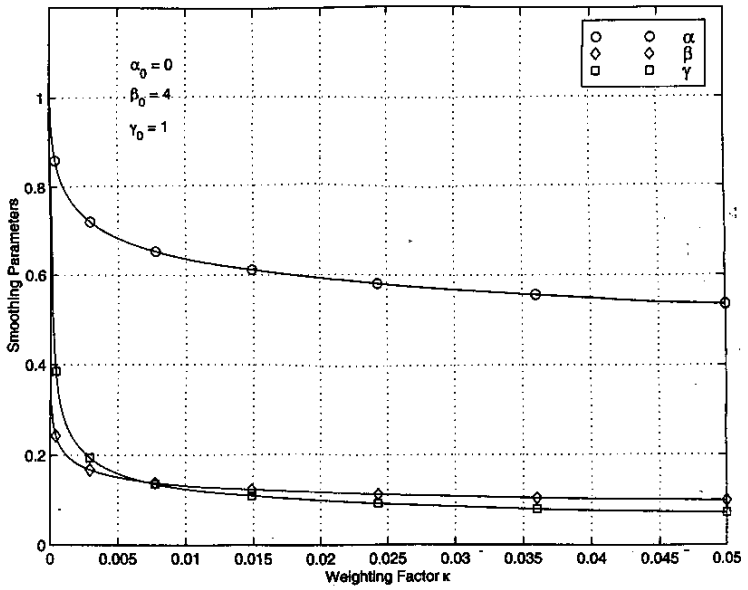

Fig. 8. Optimal solution of α, β, γ for tracking a circular path. $\alpha_0, \beta_0, \gamma_0$ are parameter values for $\kappa = 0$.

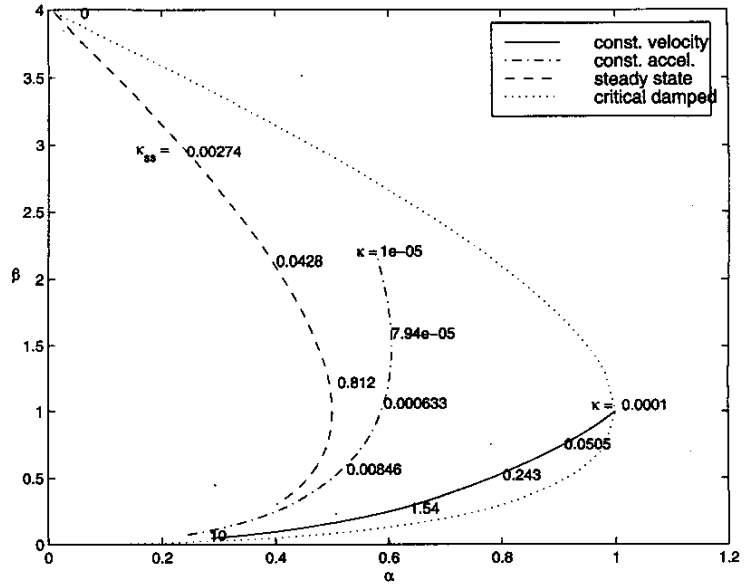

Fig. 9. Optimal solution of α and β for straight line maneuver.

case reduces to

$$f = J_{\alpha\beta,v} + \kappa\overline{x_0^2}\rho^2. \tag{40}$$

The optimal solution is obtained by searching for the parameter where the gradient of f vanishes. In this two parameter case, the following equations need to be satisfied:

$$\begin{aligned} \frac{df}{d\alpha} &= \frac{dJ_{\alpha\beta,v}}{d\alpha} + \kappa\overline{x_0^2}\frac{d(\rho^2)}{d\alpha} = 0 \\ \frac{df}{d\beta} &= \frac{dJ_{\alpha\beta,v}}{d\beta} + \kappa\overline{x_0^2}\frac{d(\rho^2)}{d\beta} = 0 \end{aligned} \tag{41}$$

which can obviously be rewritten in the matrix form as

$$\begin{bmatrix} \dfrac{dJ_{\alpha\beta,v}}{d\alpha} & \dfrac{d(\rho^2)}{d\alpha} \\ \dfrac{dJ_{\alpha\beta,v}}{d\beta} & \dfrac{d(\rho^2)}{d\beta} \end{bmatrix} \begin{bmatrix} 1 \\ \overline{\kappa x_0^2} \end{bmatrix} = G_{\alpha\beta} \begin{bmatrix} 1 \\ \overline{\kappa x_0^2} \end{bmatrix} = 0. \tag{42}$$

Equation (42) can be satisfied only if the determinant of $G_{\alpha\beta}$ is zero since the vector $[1\ \overline{\kappa x_0^2}]'$ never vanishes. Equating the determinant to zero, we can solve for β resulting in the equation:

$$\beta = \frac{\alpha^2}{2 - \alpha} \tag{43}$$

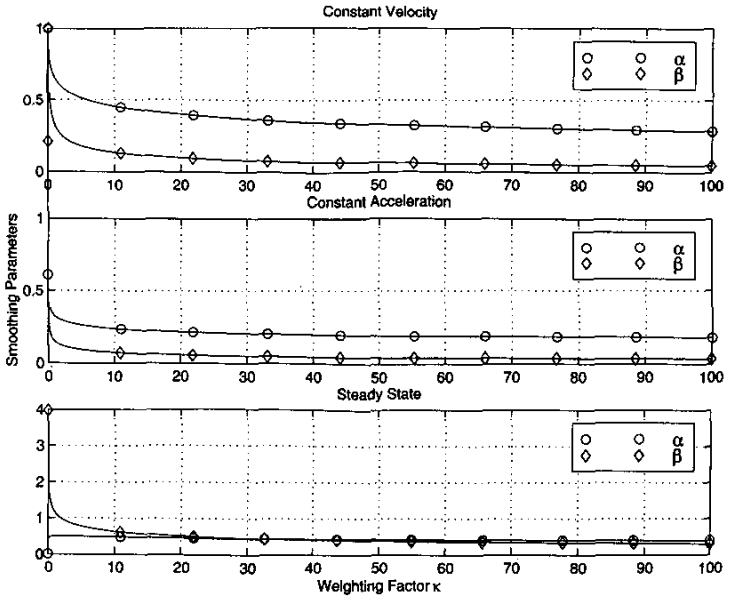

Fig. 10. Optimal solution of α and β for straight line maneuver with respect to different objectives.

which matches the optimal solution proposed by Benedict and Bordner [2]. In addition to (43), the optimal set of the parameters α and β requires satisfaction of one of (41), which for instance, is

$$0 = [2\beta(4\beta\alpha + 4\alpha^2 - 4\beta + \beta^2)]\kappa + 2v^2T^3(-\alpha^2 + 4\alpha - 4 + \beta). \quad (44)$$

This equation determines the location of the optimal parameters on the curve given by (43) as a function of the weighting factor κ. In Fig. 9 various values of the weighting factor are shown. A very small penalty on the noise ratio minimizes the settling time of the tracker, which is of course the shortest if the two poles lie at $z = 0$. This leads to the so-called dead-beat response and is given at the smoothing parameters $\alpha = \beta = 1$. Increasing the penalty of the noise ratio, moves the parameter into the underdamped region while β is decreasing. This effect has been observed in a previous discussion on the noise ratio in Section IIIA.

The optimal curve for constant acceleration is obtained by setting the initial velocity and the steady state weight to zero. Optimizing with respect to the transient response of accelerating targets results in larger values for β as shown by the dash-dot line in Fig. 9. The equation describing this curve is obtained by applying the same algorithm as for the case of constant velocity maneuver. It can be shown that the dash-dot line in Fig. 9 is described by

$$\beta_{1,2} = 3 - \tfrac{5}{2}\alpha \pm \tfrac{1}{2}\sqrt{(36 - 60\alpha + \alpha^2)} \quad (45)$$

and the second equation that needs to be satisfied is

$$0 = [4\beta^3(4\alpha^2 - 4\beta + \beta^2 + 4\beta\alpha)]\kappa + a_s^2T^5(\alpha^2 - \beta)(2\alpha - 4 + \beta)^2. \quad (46)$$

The dashed line in Fig. 9 which corresponds to a cost function including the steady state error reveals that minimizing the steady state error of the tracker by increasing the weight κ_{ss}, forces β to be maximized. The two equations describing the optimal solutions for the case where the objective function has a strong penalty on the steady state error are derived as follows:

$$\beta_{1,2} = 2 - 2\alpha \pm 2\sqrt{(1 - 2\alpha)} \quad (47)$$

$$0 = [-4\alpha^3 + (16 - 4\beta)\alpha^2 + (8\beta - \beta^2 - 16)\alpha]a_sT^2 + 8\kappa\beta^2. \quad (48)$$

For both scenarios, (45) and (47), the second derivatives have been verified to ensure local minima, whereas only one optimum reveals a lower cost.

Observing Fig. 9 reveals that better noise smoothening is obtained with smaller values of β and α, conversely, faster response is obtained with higher values of β. The special case of constant velocity has its fastest response at $\alpha = \beta = 1$. The three discussed objective functions containing constant velocity, constant acceleration and steady state are illustrated in the subplots of Fig. 10 as a function of the weight κ. A change in the variance can easily be translated into a change of the weighting factor, since these parameters appear as constants in the same cost function.

Following the aforementioned technique for optimizing the α–β filter, we design the optimal

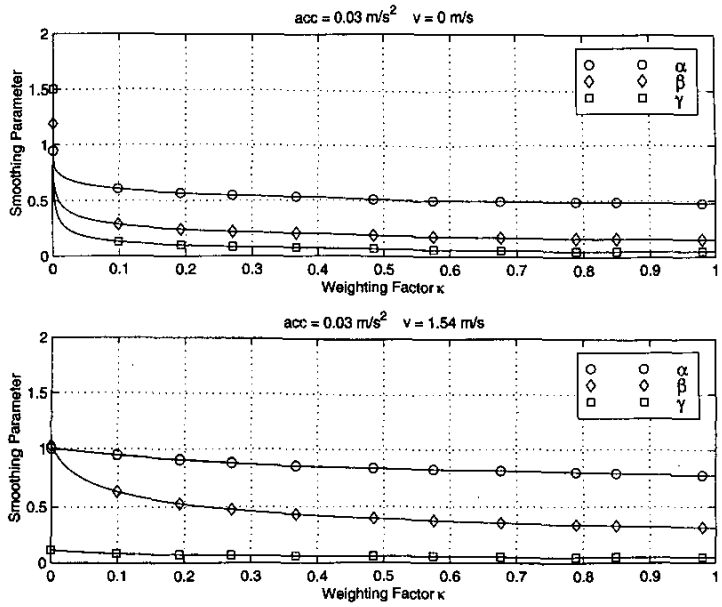

Fig. 11. Optimal solution of α,β,γ for straight line maneuver with two different cost functions.

α–β–γ filter. The equation of the transient error cost functions of an α–β–γ tracker is also divided in two fractions depending only on the velocity and the acceleration. Two sets of the optimal smoothing parameters are shown in Fig. 11, which have been derived by the constrained parameter optimization algorithm. The upper plot uses a constant acceleration input without initial velocity, whereas the lower plot shows the optimal solution for a combined cost function with an acceleration of 0.03 m/s^2 and a velocity of 3 knots. As also observed in Fig. 9, higher parameters cause a faster system response. Conversely, for better noise smoothing, the optimal parameters are decreasing. A closed-form expression of the optimal set of parameter can be derived for a straight line target trajectory where the target is accelerating. The gradient matrix of the cost function with respect to a, b, and c is

$$\begin{vmatrix} \frac{dJ_{abc,v}}{da} & \frac{dJ_{abc,a}}{da} & \frac{d(\rho^2)}{da} \\ \frac{dJ_{abc,v}}{db} & \frac{dJ_{abc,a}}{db} & \frac{d(\rho^2)}{db} \\ \frac{dJ_{abc,v}}{dc} & \frac{dJ_{abc,a}}{dc} & \frac{d(\rho^2)}{dc} \end{vmatrix} \begin{bmatrix} 1 \\ 1 \\ \overline{\kappa x_0^2} \end{bmatrix} = G_{abc} \begin{bmatrix} 1 \\ 1 \\ \overline{\kappa x_0^2} \end{bmatrix} \tag{49}$$

where the previously introduced transformation into the a-b-c space is carried out (equation (9)). Equating the determinant of G_{abc} to zero and solving for the parameter b, leads to the optimal solution in the a-b-c space:

$$b_1 = \frac{(1+c)^2(a-1)+a^2c}{c(2-a)} \tag{50}$$

$$b_2 = \frac{(1+c)(c+1-a)}{c}. \tag{51}$$

It can be seen that b_1 reduces to the optimal solution of the α–β filter (equation (43)) if $c=-1$, whereas b_2 vanishes for this case. The two additional conditions to be satisfied cannot easily be simplified. Furthermore, to ensure the optimality of the solution the parameter resulting in the smaller cost is selected.

The optimal solutions of the α, β and γ parameters are derived for a constant initial velocity and changing acceleration of a target moving along a straight line. The objective function for this case consists of the transient maneuver error cost equation (37), and the prediction noise-ratio equation (18). We arrive at the optimal solutions shown in Fig. 12 by using a numerical optimization during which the positive-definiteness of the Hessian evaluated at the optimal parameter b_1 and b_2 has been verified. The positive-definiteness of the Hessian for the solutions (50) and indefiniteness for (51) implies that one is a global minimum b_1 and the other is a saddle b_2. Fig. 12 shows the change of the smoothing parameters versus the acceleration. It can be observed that for zero acceleration, the filter reduces to the α–β filter since the α–β filter is able to track a nonaccelerating target. Increasing the acceleration results in increasing γ and since the rate of changing the velocity increases, β also increases.

V. CONCLUSION

This paper focuses on the design of α–β–γ filters. The issue of the determination of the stability volume

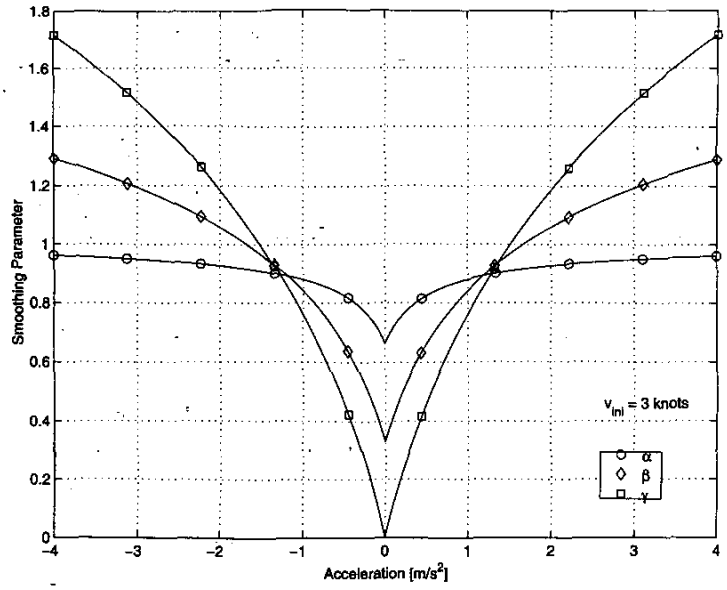

Fig. 12. Optimal α,β,γ parameters at constant sensor noise and changing acceleration.

TABLE I
Jury's Stability Table of α–β–γ Filter

Row	z^0	z^1	z^2	z^3
1	$\alpha-1$	$-2\alpha-\beta+\frac{1}{4}\gamma+3$	$\alpha+\beta+\frac{1}{4}\gamma-3$	1
2	1	$\alpha+\beta+\frac{1}{4}\gamma-3$	$-2\alpha-\beta+\frac{1}{4}\gamma+3$	$\alpha-1$
3	$\alpha(\alpha-2)$	$\alpha(4-2\alpha-\beta+\frac{1}{4}\gamma)-\frac{1}{2}\gamma$	$\alpha(\alpha+\beta-2+\frac{1}{4}\gamma)-\frac{1}{2}\gamma$	—

is first addressed. A simple technique to simplify the procedure to determine the stability bounds on the α, β, and γ filters is proposed. This includes parameterizing the characteristic equation of the α–β–γ filter via a nonlinear transformation to what is referred to as the *a-b-c* space. In this space, the characteristic equation appears to be the product of the characteristic equation of an α–β filter and a first order pole which is only a function of the parameter c. One can now easily determine the bounds on the parameters with knowledge of the bounds on the parameters of an α–β filter. Therefore, the stability volume in the *a-b-c* space is a prism which can be transformed into the α–β–γ space. To quantify the performance of α–β–γ filters, various metrics are defined such as the noise ratio which is a figure of demerit to represent the noise filtering capability of the tracker. A closed-form solution to the noise ratio is arrived at in the α–β–γ space which reduces to the noise ratio for the α–β filter when γ is equated to zero. The resulting solution is shown to be different from that derived in the literature. Numerical simulations are carried out to evaluate the veracity of the derived solution. Closed-form equations to characterize the transient performance of the α-β–γ tracker for straight line and circular maneuvers are also derived. These are subsequently used in conjunction with the noise ratio to determine the optimal set of the tracker parameters based on a cost function which is a weighted combination of the noise ratio, the transient response metric and the steady state error. Variation of the tracker parameters for different weights of the cost function are studied to provide the designer with information for the optimal selection of the α, β, and γ parameters.

APPENDIX

A. Jury's Stability Test of α–β–γ Filter

The Jury's Table constructed from the coefficients of the characteristic polynomial (equation (52)) of nth-order yields Table I

$$P(z) = a_0 z^n + a_1 z^{n-1} + \cdots + a_{n-1} z + a_n. \quad (52)$$

The *Jury's stability criterion* requires a set of constraints to be satisfied. The condition $a_0 > 0$ is satisfied for the α–β–γ filter since $a_0 = 1$. To satisfy the constraint $|a_n| < a_0$, the criterion requires $|\alpha - 1| < 1$, which is equivalent to

$$0 < \alpha < 2. \quad (53)$$

Substituting $z = 1$ and applying the constraint $P(z)|_{z=1} > 0$, requires satisfaction of the inequality

TABLE II
Square of Noise Ratios According to Different Approaches

	Sklansky	Benedict & Bordner	Tenne & Singh
Prediction Noise Ratio ρ_p^2	$\frac{6\alpha^2-3\alpha\beta+6\beta-\beta^2}{3\alpha(4-2\alpha-\beta)}$	—	$\frac{2\alpha^2+\alpha\beta+2\beta}{\alpha(4-2\alpha-\beta)}+\frac{4\beta\gamma}{\alpha(4-2\alpha-\beta)(4\alpha\beta+\alpha\gamma-2\gamma)}$
Update Noise Ratio ρ_s^2	—	$\frac{2\alpha^2-3\alpha\beta+2\beta}{\alpha(4-2\alpha-\beta)}$	$\frac{2\alpha^2-3\alpha\beta+2\beta}{\alpha(4-2\alpha-\beta)}+\frac{4\beta\gamma(1-\alpha)^2}{\alpha(4-2\alpha-\beta)(4\alpha\beta+\alpha\gamma-2\gamma)}$
Simulation			for $\gamma=0$:
$\rho_p^2=1.9540$	$\rho_p^2=1.2058$	—	$\rho_p^2=1.9565$
$\rho_s^2=0.7398$	—	$\rho_s^2=0.7391$	$\rho_s^2=0.7391$

Note: Results are obtained with $\alpha=0.5$ and $\beta=0.7$.

$$1+(\alpha+\beta+\tfrac{1}{4}\gamma-3)+(-2\alpha-\beta+\tfrac{1}{4}\gamma+3)+\alpha-1>0$$

which can be rewritten as

$$\gamma>0. \tag{54}$$

Satisfying the constraint $P(z)|_{z=-1}<0$, for odd n, yields

$$2\alpha+\beta<4 \tag{55}$$

which is the same constraint for α and β as the α–β filter. The last condition that $|b_2|>|b_0|$, where

$$b_k=\begin{vmatrix} a_n & a_{n-1-k} \\ a_0 & a_{k+1}\end{vmatrix}, \qquad k=0,1,2,\ldots,n-1 \tag{56}$$

is used to construct the third row of Table I, requires

$$|\alpha(\alpha-2)|>|\alpha(\alpha-2)+\alpha(\beta+\tfrac{1}{4}\gamma)-\tfrac{1}{2}\gamma|. \tag{57}$$

Observing (57) and knowing the fact that $\alpha(\alpha-2)$ is always negative within the stability area, we have

$$\alpha(\beta+\tfrac{1}{4}\gamma)-\tfrac{1}{2}\gamma>0.$$

This statement leads to the constraint on γ for which the α–β–γ tracker is stable, which is

$$\gamma<\frac{4\alpha\beta}{2-\alpha}. \tag{58}$$

B. Derivation of Square of Noise Ratio

The square of the noise ratio is coincident with the $(1,1)$ element of the covariance matrix divided by the input noise variance. The elements of the symmetric covariance matrix are

$$\hat{P}=\begin{bmatrix} p_1 & p_2 \\ p_2 & p_3\end{bmatrix}. \tag{59}$$

The steady state solution of (17) can be obtained by writing:

$$\hat{P}_{ss}(k)=\Phi(I-KC)\hat{P}_{ss}(k)(I-KC)^T\Phi^T+\Phi K\sigma_0^2K^T\Phi^T. \tag{60}$$

and equating the elements on the left and right side, thus obtaining three equations for the three unknown elements of $\hat{P}$. Employing a symbolic solver returns the following covariance matrix:

$$\hat{P}_{ss}=\sigma^2\begin{bmatrix} \frac{(2\beta+\alpha\beta+2\alpha^2)}{\alpha(4-\beta-2\alpha)} & \frac{\beta(2\alpha+\beta)}{\alpha T(4-\beta-2\alpha)} \\ \frac{\beta(2\alpha+\beta)}{\alpha T(4-\beta-2\alpha)} & \frac{2\beta^2}{T^2\alpha(4-\beta-\alpha)}\end{bmatrix}. \tag{61}$$

The square of the prediction noise ratio is then obtained by

$$\rho_p^2=C\hat{P}_{ss}C^T/\sigma^2 \tag{62}$$

$$=\frac{2\alpha^2+\alpha\beta+2\beta}{\alpha(4-2\alpha-\beta)}. \tag{63}$$

C. Numerical Simulation of Noise Ratio

To prove the veracity of (18), numerical simulations are carried out. Results of simulating an α–β filter for normally distributed white noise are used to calculate the noise ratio by calculating the ratio of the rms value of the output and input. Table II summarizes the different solutions for the square of the noise ratio and displays the simulation result for the parameter set $\alpha=0.5$ and $\beta=0.7$. As is clear from the table, the solution of Sklansky does not match the results of the simulation while (18) matches the simulated results. Sklansky's sampled continuous model differs from the discrete representation used in this work. In addition, the update noise ratio derived by Benedict and Bordner is shown in Table II and matches the numerical results.

DIRK TENNE
TARUNRAJ SINGH
Department of Mechanical and Aerospace Engineering
SUNY Buffalo
1009 Furnas Hall
Buffalo, NY 14260
E-mail: (tenne@eng.buffalo.edu)
(tsingh@eng.buffalo.edu)

REFERENCES

[1] Sklansky, J. (1957)
Optimizing the dynamic parameter of a track-while-scan system.
RCA Laboratories, Princton, NJ, June 1957.

[2] Benedict, T. R., and Bordner, G. W. (1962)
Synthesis of an optimal set of radar track-while-scan smoothing equations.
IRE Transactions on Automatic Control, **AC-1** (July 1962).

[3] Simpson, H. R. (1962)
Performance measures and optimization condition for a third order sampled-data tracker.
IEEE Transactions on Automatic Control, **AC-12** (June 1962).

[4] Neal, S. R. (1967)
Parametric relations for α–β–ν filter predictor.
IEEE Transactions on Automatic Control, **AC-12** (June 1967).

[5] Kanyuck, A. J. (1970)
Transient response of tracking filters with randomly interrupted data.
IEEE Transactions on Aerospace and Electronic Systems, **AES-6**, 3 (May 1970).

[6] Schooler, C. C. (1975)
Optimal α–β filters for systems with modeling inaccuracies.
IEEE Transactions on Aerospace and Electronic Systems, **AES-11** (Nov. 1975).

[7] Friedland, B. (1973)
Optimal steady-state position and velocity estimation using noisy sampled data.
IEEE Transactions on Aerospace and Electronic Systems, **AES-9** (Nov. 1973).

[8] Fitzgerald, R. J. (1980)
Simple tracking filters: Steady-state filtering and smoothing performance.
IEEE Transactions on Aerospace and Electronic Systems, **AES-16** (May 1980).

[9] Gleason, D., and Andrisani, D. (1988)
Constant gain analysis for discrete tracking filters.
IEEE NAECON, 1988.

[10] Sudano, J. J. (1993)
The α–β–γ tracking filter with a noisy jerk as the maneuver model.
IEEE Transactions on Aerospace and Electronic Systems, **29**, 2 (Apr. 1993).

[11] Singer, R. A. (1970)
Estimating optimal tracking filter performance for manned maneuvering targets.
IEEE Transactions on Aerospace and Electronic Systems, **AES-5** (Nov. 1970).

[12] Arcasoy, C. C., and Ouyang, G. (1997)
Analytical solution of the α–β–γ tracking filter with a noisy jerk as correlated target maneuver model.
IEEE Transactions on Aerospace and Electronic Systems, **33** (Jan. 1997).

[13] Kalata, P. R. (1984)
The tracking index: A generalized parameter for α–β and α–β–γ target trackers.
IEEE Transactions on Aerospace and Electronic Systems, **AES-20**, 2 (Mar. 1984).

[14] Ekstrand, B. (2001)
Poles and zeros of α–β and α–β–γ tracking filters.
IEE Proceedings on Control Theory Application, **148**, 5 (Sept. 2001), 370–376.

[15] Gray, J. E., and Murray, W. (1993)
A derivation of an analytic expression for the tracking index for the alpha-beta-gamma filter.
IEEE Transactions on Aerospace and Electronic Systems, **29**, 3 (July 1993).

[16] Alouani, A. T., Xia, P., Rice, T. R., and Blair, W. D. (1991)
A two-stage Kalman estimator for state estimation in the presence of random bias and tracking maneuvering targets.
In *Proceedings of IEEE Conference on Decision and Control*, **2** (1991).

[17] Alouani, A. T., Xia, P., Rice, T. R., and Blair, W. D. (1992)
A two-stage Kalman estimator for tracking maneuvering targets.
In *Proceedings of IEEE International Conference on Systems, Man., and Cybernetics*, **2** (1991).

[18] Blair, W. D. (1992)
Two-stage alpha-beta-gamma estimator for tracking maneuvering targets.
In *ACC*, Weapons Control Division, Naval Surface Warfare Center, Dahlgren, VA, 1992.

[19] Blair, W. D., and Watson, G. A. (1992)
Two-stage alpha-beta-gamma-lambda estimator for tracking constant speed, maneuvering targets.
In *ACC*, Weapons Control Division, Naval Surface Warfare Center, Dahlgren, Virginia, 1992.

[20] Soong, T. T. (1981)
Probabilistic Modeling and Analysis in Science and Engineering.
New York: Wiley, 1981.

[21] Ogata, K. (1987)
Discrete-Time Control Systems.
Englewood Cliffs, NJ: Prentice-Hall, University of Minnesota, 1987.

Gating Techniques for Maneuvering Target Tracking in Clutter

Gating techniques for maneuvering target tracking using an IMM-PDA filter are considered in this paper. Existing gating techniques, namely, Centralized Gating and Model Based Gating are reviewed and new gating techniques, called Model Probability Weighted Gating and Two-Stage Model Probability Weighted Gating, are proposed. A benchmark trajectory and a random scenario are considered for performance evaluation of the gating techniques in terms of RMS errors, percentage of track loss and computational load.

I. INTRODUCTION

Tracking a maneuvering target in clutter is important in many applications. However clutter

Manuscript received June 8, 2001; revised April 18, 2002; released for publication May 13, 2002.

IEEE Log No. T-AES/38/3/06453.

Refereeing of this contribution was handled by P. K. Willett.

This work is supported by Defence Science Technology Organization (DSTO), the Center for Sensor Signal and Information Processing (CSSIP) and the University of Melbourne.